



# Influence of cyclical mechanical strain on extracellular matrix gene expression in human lamina cribrosa cells in vitro

Ruaidhrí P. Kirwan,<sup>1</sup> Cecilia H. Fenerty,<sup>2</sup> John Crean,<sup>1</sup> Robert J. Wordinger,<sup>3</sup> Abbot F. Clark,<sup>4</sup> Colm J. O'Brien<sup>1,2</sup>

<sup>1</sup>Conway Institute of Biomolecular and Biomedical Research University College Dublin, Dublin, Ireland; <sup>2</sup>Institute of Ophthalmology, Mater Misericordiae University Hospital, Dublin, Ireland; <sup>3</sup>Department of Cell Biology and Genetics, University of North Texas Health Center at Fort Worth, Fort Worth, TX; <sup>4</sup>Glaucoma Research, Alcon Research Ltd., Fort Worth, TX

**Purpose:** The mechanical effect of raised intraocular pressure is a recognised stimulus for optic neuropathy in primary open angle glaucoma (POAG). Characteristic extracellular matrix (ECM) remodelling accompanies axonal damage in the lamina cribrosa (LC) of the optic nerve head in POAG. Glial cells in the lamina cribrosa may play a role in this process but the precise cellular responses to mechanical forces in this region are unknown. The authors examined global gene expression profiles in lamina cribrosa cells exposed to cyclical mechanical stretch, with an emphasis on ECM genes.

**Methods:** Glial fibrillary acid protein negative primary LC cells were generated from the optic nerve head tissue of three normal human donors. Confluent cell passages (n=4) were exposed to 15% stretch at 1 Hz or static conditions for 24 h using the Flexercell system. Gene expression was assessed using Affymetrix U133A microarrays with pooled RNA. Expression levels were normalized using robust multi-chip average (RMA). Expression data was annotated using NIH DAVID software. ECM-related gene expression was validated in an independent experiment using quantitative real-time PCR and protein synthesis was measured using ELISA and immunohistochemistry.

**Results:** Compared with static controls, 805 genes were upregulated and 644 were downregulated by  $\pm 1.5$  fold in stretched LC cells. Gene ontologies included ECM, cell proliferation, growth factor activity, and signal transduction. Differentially expressed ECM genes included elastin, collagens (IV, VI, VIII, IX), thrombospondin 1, perlecan, and lysyl oxidase. Quantitative PCR demonstrated that the expression of TGF- $\beta$ 2, BMP-7, elastin, collagen VI, biglycan, versican, EMMPRIN, VEGF, and thrombospondin were reproducible and consistent with the microarray data. VEGF and TGF- $\beta$ 2 protein levels were also significantly ( $p < 0.05$ ) increased in stretched cell media supernatants. Immunohistochemistry demonstrated increased EMMPRIN (an extracellular matrix metalloproteinase inducer) protein in human POAG optic nerve head tissue compared to nonglaucomatous controls.

**Conclusions:** These findings demonstrate that LC cells respond to mechanical stimuli in vitro by transcription of several components and modulators of the ECM. Some of the upregulated ECM genes identified are novel in the context of glaucomatous optic neuropathy (biglycan, versican, EMMPRIN, and BMP-7). The LC cell may represent both an important pro-fibrotic cell type in the optic nerve head and an attractive target for novel therapeutic intervention in POAG.

The lamina cribrosa is a distinct histological region of the optic nerve head (ONH). It is composed of approximately ten perforated (cribriform) connective tissue plates that permit the passage of retinal ganglion cell axons as they exit the ONH [1]. It is a compliant tissue, which in normal human eyes sustains changes in intraocular pressure (IOP) without loss of structural or morphological integrity. This compliance reduces markedly with age due to increased collagen and reduced proteoglycan content in the lamina cribrosa extracellular matrix (ECM) [2,3]. Two important cell types that have been characterized in the lamina cribrosa include the ONH astrocyte and the lamina cribrosa (LC) cell. Both are members of the glial population of the ONH, however, the LC cell, unlike the astrocyte, does not express glial fibrillary acid protein (GFAP) [4]. In terms of morphology, LC cells are broad, flat and polygonal, distinguishing them from the ONH astrocytes which are star shaped [5]. ONH astrocytes are found

throughout the ONH and separate the retinal ganglion cell axons from the cribriform plates. The LC cells, in contrast, are localized to the lamina cribrosa region and are situated within or between the cribriform plates [6].

Primary open angle glaucoma (POAG) is a progressive optic neuropathy characterized by raised IOP, retinal ganglion cell (RGC) axon loss, and excavation or cupping of the optic nerve head [7]. It affects over 60 million people worldwide, representing one of the most common causes of irreversible blindness [8]. Electron micrograph and immunohistochemistry studies demonstrate marked disruption to ECM architecture and composition in the glaucomatous lamina cribrosa. This includes backward displacement and distortion of the cribriform plates with increased amounts of collagen VI, elastin, and transforming growth factor- $\beta$ 2 [9-12]. Such ultrastructural changes may adversely affect the biomechanical properties of the lamina cribrosa, predisposing it to collapse as the IOP rises. An obvious consequence of lamina cribrosa collapse is the compression of RGC axons, which arrests their axoplasmic flow. This is clearly demonstrated in models of POAG in monkeys [13]. It is likely that this is also the case in humans

Correspondence to: Dr. Ruaidhrí Kirwan, Institute of Ophthalmology, Mater Misericordiae University Hospital, No. 60 Eccles Street, Dublin 7, Ireland; email: ruaidhri.kirwan@ucd.ie

with POAG, offering a rational explanation for the interruption of optic nerve function and characteristic visual field disturbances. More recently, studies in monkeys have proposed that these mechanical insults to optic nerve function occur early in POAG, and support the hypothesis that the primary pathogenic event is mechanical failure of the lamina cribrosa [14].

It is not yet known which cell type is principally involved in ECM remodeling in the optic nerve head in POAG, however, the ONH astrocytes and LC cells have been implicated [6]. One of the triggers for ECM remodeling may be the backward displacement of the lamina cribrosa (due to elevated IOP) which will deform and stretch its resident cells. Previous studies have shown that ONH astrocytes respond to hydrostatic pressure by upregulating elastin and heat shock protein-27 synthesis and that LC cells respond to hydrostatic pressure by upregulating collagen I mRNA synthesis or to cyclical strain by upregulation of TGF- $\beta$ 1 mRNA synthesis, TGF- $\beta$ 1 protein, and matrix metalloproteinase-2 activity [15-18]. These findings demonstrate a mechanosensory capability in both cell types which respond by release of components or modulators of the ECM. Unlike the LC cell, however, the ONH astrocyte has also been shown to release the neurotoxic mediator NO synthase-2 and may therefore directly induce axonal death in the optic nerve head [19].

While raised IOP is an established macro-stimulus for cupping of the ONH in POAG, the discrete transcriptional responses to mechanical forces in the lamina cribrosa in vivo are less clear. The emergence of microarray technology, which allows large scale profiling of gene expression in biological systems, has greatly enhanced our capacity to probe the molecular pathogenesis of POAG [20]. In this present study, using microarrays, global changes in the LC cell transcriptome in response to 24 h of cyclical mechanical stretching were examined. Changes in selected ECM gene expression were then confirmed by quantitative PCR and corresponding protein changes by ELISA and immunohistochemistry. Some of the proteins of these genes have previously been characterized in the optic nerve head in POAG (e.g., collagen VI, elastin, and TGF- $\beta$ 2) whereas others are novel in this context (e.g., EMMPRIN, biglycan, VEGF, and BMP-7).

## METHODS

**Cell culture:** Primary cultures of human LC cells were generated from carefully dissected optic nerve head tissue from three normal donors and characterized as reported previously [5,21]. Cultures were confirmed to be glial fibrillary acid protein (GFAP) negative and maintained in 5% CO<sub>2</sub>-95% air at 37 °C. Four separate cultures of confluent cells were used for four mechanical stretching experiments (n=4). Each passage of cells was trypsinized and seeded equally (6x10<sup>4</sup> cells per well) in duplicate to flexible six well culture plates coated with laminin (Flexcell International Corp., Hillsborough, NC). Confluent monolayers formed every 7-10 days. Two cultures of cells were generated from donor 1 and one culture from donor 2 (total of 3 separate cultures), which were then used for the microarray analysis (Figure 1). A separate fourth culture of cells was generated from donor 3 and used for real-

time PCR validation (Figure 1). All cultures used were between cell passages four and six. Cell media supernatants from all four experiments (n=4) were removed for analysis by enzyme linked immunosorbent assay (ELISA).

**Application of cyclical mechanical stretch:** Confluent LC cells were stretched using the Flexercell® Tension Plus™ FX-4000T system (Flexcell International Corp.) [22]. This is a computer driven apparatus that creates a programmable bi-axial strain across laminin coated culture wells when positioned on a vacuum base station (Figure 2A). Control plates, also flexible and laminin coated, are not positioned on the base station but instead are placed adjacent to it in the same incubator. Each cycle of strain contains an upstroke to the predetermined percentage elongation and then falls to baseline (0% strain) with a distinct dirotic notch (Figure 2B). Confluent cells were serum starved for 24 h prior to 1 s cycles (1 Hz) of 15% strain or static conditions for 24 h. All cells were maintained in 5% CO<sub>2</sub>-95% air at 37 °C for the duration of the experiment.

**Isolation of RNA:** Total RNA was isolated using a silica gel-based RNeasy spin column protocol (Qiagen, Valencia, CA). Total RNA was suspended in 30  $\mu$ l of RNase-free H<sub>2</sub>O. RNA concentrations and purity were calculated from the absorbance at 260/280 nm and 5  $\mu$ g of each sample was resolved on 1.5% agarose gels to assess their integrity.

**Microarray analysis:** To investigate the effect of 24 h of cyclical mechanical stretching on global gene expression in LC cells, Affymetrix HG-U133A microarrays containing 22,283 oligonucleotide target probes were used. Complementary DNA (cDNA) was synthesized from total RNA using SuperScript Choice kit (Invitrogen, Paisley, UK). Biotin-labeled cRNA was prepared from template cDNA in an in vitro transcription (IVT) reaction using the Bioarray High-Yield RNA transcript labeling kit (Enzo Life Sciences, Farmingdale, NY). Labeled RNA from three separate stretch and control experiments (n=3) was pooled and then hybridized to an experimental or control microarray. Arrays were washed and fluorescently labeled before being scanned by a confocal laser scanner. Raw image files (CEL format) were obtained through Affymetrix Suite 5.0 software (MAS 5.0). Probe intensities from the two chips were then normalized by robust multi-chip analysis (RMA) using RMA Express. RMA Express is a stand alone graphic user interface package that analyzes directly from the Affymetrix microarray image file (CEL format) and comprises of a number of steps to background adjust, quantile normalize, log transform, and summarize the perfect match probe values [23]. This form of normalization is called "complete normalization" as it uses the probe intensity data from all arrays in an experiment to form the normalizing relation. Expression data was filtered using Microsoft Excel. Genes displaying a signal log ratio of greater than 0.6 or less than -0.6 ( $\pm$ 1.5 fold) were retained for further analysis and a subset of ECM/ECM-related genes were selected for independent validation by real time PCR.

**Bio-informatic analysis:** Biologically relevant groups from the microarray data were generated using the Database for Annotation, Visualization and Integrated Discovery

(DAVID; version 1.0) from the National Institutes of Health [24]. This is a web-based software package that functionally annotates a list of uploaded gene identifiers and converts them into an ordered table of biological themes.

**Quantitative real-time PCR:** Total RNA (1 µg) was used to synthesize the first-strand cDNA using random hexamers and SuperScript II reverse transcriptase (Invitrogen, Paisley, UK). The cDNA was used for quantitative real-time PCR amplification with TaqMan™ chemistry (Applied Biosystems, Foster City, CA). Fluorogenic probes and sequence specific primers for TGF-β2, BMP-7, elastin, collagen VI, biglycan, versican, EMMPRIN, thrombomodulin, VEGF, and the endogenous control 18S ribosomal RNA were designed and optimized in a preformulated assay (Assay-on-Demand™, Applied Biosystems). The target gene names, Unigene identifiers and Applied Biosystems primer/probe assay identifiers are shown in Table 1. Duplicate cDNA template samples were amplified and analyzed in the Prism 7900HT sequence detection system (Applied Biosystems). Thermal cycler conditions were 10 min at 95 °C followed by 40 cycles of 30 s at 95 °C to denature the DNA and 30 s at 60 °C to anneal and extend the template. A standard curve of cycle thresholds using serial dilutions of cDNA samples were established and used to calculate the relative abundance of the target gene between stretch and control samples. Values were normalized to the relative amounts of 18S mRNA, which were obtained from a similar standard curve.

**Enzyme linked immunosorbent assay (ELISA):** For quantification of total TGF-β2 or VEGF protein in stretched and static cell media supernatants (n=4), the quantitative sandwich immunoassay technique was used (both ELISA kits, R&D Systems, Minneapolis, MN). They were activated where appropriate with 1 N HCl according to the manufacturers instructions and standard concentrations of TGF-β2 or VEGF protein were prepared. Activated samples and standards were loaded to separate 96 well plates coated with monoclonal antibodies specific for human TGF-β2 or VEGF. After washing away any unbound substances, an enzyme-linked polyclonal antibody specific for TGF-β2 or VEGF was added to the wells. Following a second wash to remove any unbound antibody-enzyme reagent, a solution of hydrogen peroxide and tetramethylbenzidine was added to the wells after which a blue color developed in proportion to the amount of target protein bound in the initial step. The reaction was stopped using sulfuric acid and the optical density of each well was measured at 450 nm.

**Double immunofluorescence histochemistry:** Eyes from three human donors were obtained from regional eye banks and placed in 4% neutral buffered formalin within 4 h of death. Two of the donors had a documented history of glaucoma. The third donor had no history of ocular disease (normal control). The posterior segments were embedded in paraffin and 6 µm optic nerve head sections were cut and mounted on glass slides. After paraffin removal, the tissue was quenched for aldehydes by treatment in a 0.05 M glycine (Sigma, Dorset, UK) solution for 15 min. Nonspecific binding sites were then blocked for 15 min with phosphate buffered saline (PBS) so-

lution containing 1% BSA and 1% serum from the species (rabbit or mouse) in which the secondary antibody was raised. The slides were washed in PBS prior to incubation with a mixture of anti-EMMPRIN antibody (diluted 1:25 in PBS; Abcam, Cambridge, MA) and anti-GFAP antibody (diluted 1:80 in PBS; Sigma, Dorset, UK) at 4 °C overnight. The sections were then washed 3 times in PBS. For detection of EMMPRIN, the sections were incubated with Alexa Fluor-488 labeled anti-mouse IgG for 1 h at room temperature (RT). For detection of GFAP, the sections were incubated with Alexa Fluor-594 labeled anti-rabbit IgG for 1 h at RT (both secondary antibodies were obtained from Molecular Probes, Leiden, The Netherlands). The tissue nuclei were then DAPI stained (300 nM in water) for 5-10 min. Images were captured with a Nikon Microphot FXA (Nikon, Inc., Melville, NY) equipped with a SenSys CCD camera (Photometrics, Tucson, AZ). Images were deconvoluted using Scanalytics IPLAB (Scanalytics, Fairfax, VA) and Vaytek Microtome (Vaytek, Fairfield, IA) software.

**Statistical analysis:** Data for the ELISA are summarized as the mean fold change±standard error (SE) calculated from four separate experiments (n=4). The paired student t-test was used to analyze the statistical significance (p<0.05) of differences between mean values.

## RESULTS

**Microarray and bioinformatic analysis:** To investigate the effects of cyclical mechanical stretch on global gene expression in LC cells we used Affymetrix HG-U133A cRNA microarrays. A series of three cell culture experiments were performed generated from two separate human donors. Figure 3A shows a box plot of the control and stretch microarrays following normalization by Robust Multichip Analysis (RMA). The microarray data discussed in this manuscript is available at the Gene Expression Omnibus (GEO) database under the accession number GSE3166. Figure 3B shows the log/log pairwise scatter plot of the expression levels of the 22,283 genes from stretch and control arrays. Of the 22,283 genes scanned, 805 were upregulated by more than 0.6 signal log ratios (1.5 fold) and 644 were downregulated by more than -0.6 signal log ratios (1.5 fold) in stretch compared to control. In order to generate biologically relevant groups of genes from the microarray data, we used the NIH DAVID software. This separated the genes into three broad functional groups; biological process, molecular function, and cellular component (Figure 4). In Table 2 we list individual differentially expressed genes belonging to the categories of ECM, cell proliferation, growth factor activity, cell surface receptor linked signal transduction, and coagulation. These categories have been shown in detail, as they are the categories to which the nine validated genes belong. Of particular interest to our work was the ECM category, which showed that 30 ECM genes were differentially expressed in stretch compared to control (24 upregulated, 6 downregulated, Table 2). Components of the ECM within this category included elastin, biglycan, perlecan, collagen IV, collagen VI, collagen VIII, collagen IX, and collagen XIV. Modulators of the ECM within this category included

ADAMTS2, ADAMTS9, lysyl oxidase, MMP-23A, and thrombospondin 1.

**Quantitative real time PCR:** To validate the microarray analysis, we performed quantitative real-time PCR with TaqMan™ chemistry using independent RNA (not used for the microarray analysis) from stretched and control LC cells generated from a third human donor. We analyzed 9 genes whose expression was upregulated (TGF- $\beta$ 2, BMP-7, elastin, collagen VI, biglycan, versican, and VEGF) or downregulated (thrombomodulin) in response to 24 h of cyclical mechanical stretch. While not all genes validated were assigned to the ECM category (TGF- $\beta$ 2, VEGF, BMP-7, EMMPRIN, and thrombomodulin) their functions do include maintenance or regulation of ECM metabolism. Figure 5A shows the fold expression changes observed using real-time PCR for the 9 validated genes. The results showed that the expression changes for all selected genes were reproducible and consistent with the direction of change predicted by microarray analysis. The magnitude of change determined by microarray and real-time PCR were somewhat different, a result which was not surprising considering the technical differences in the methods of analysis and normalization.

**Enzyme linked immunosorbent assay (ELISA):** To investigate if the changes in mRNA reflected similar changes in protein synthesis, we used enzyme linked immunosorbent assay (ELISA). VEGF and TGF- $\beta$ 2 were chosen as representative genes whose expression was altered by cyclical mechanical stretch. Figure 5B shows that VEGF and TGF- $\beta$ 2 protein secretion were significantly increased in cell media supernatants of stretched LC cells compared to static controls. Mean control TGF- $\beta$ 2 concentration was  $87 \pm 19$  pg/ml (SE) and mean stretch TGF- $\beta$ 2 concentration was  $115 \pm 30$  pg/ml (SE; n=4;

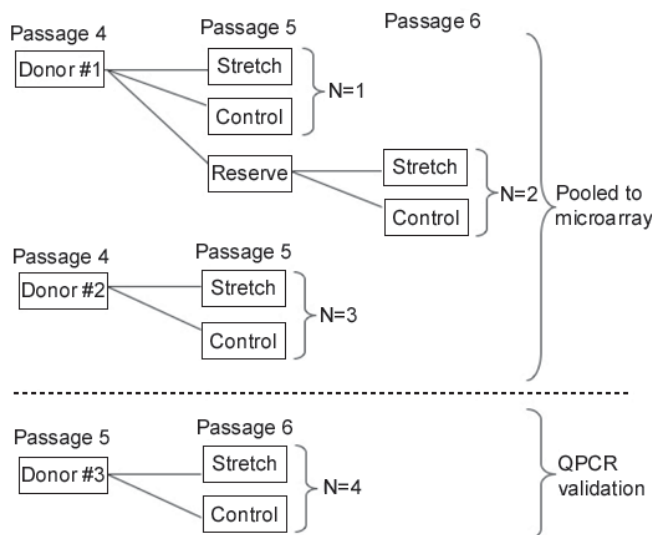


Figure 1. Cell culture experimental design. Four separate passages of lamina cribrosa (LC) cells (n=4) were generated from three human donors. Three passages of cells from donors 1 and 2 were used for the microarray analysis (pooled; n=3) and the fourth passage of cells from donor 3 was used for the real time PCR validation. All experiments were conducted on LC cells between passages 4 and 6.

p=0.02). Mean control VEGF concentration was  $241 \pm 66$  pg/ml (SE) and mean VEGF stretch concentration was  $407 \pm 148$  pg/ml (SE; n=4; p=0.03). This correlated with the recorded direction of change in VEGF and TGF- $\beta$ 2 mRNA synthesis as measured by microarray and real-time PCR.

TABLE 1. APPLIED BIOSYSTEMS PRIMER AND PROBE ASSAY IDENTIFIERS (ASSAY-ON-DEMAND™)

Gene	Unigene ID	Primer & probe assay ID
Elastin	Hs.252418	Hs00355783_m1
BMP-7	Hs.170195	Hs00233477_m1
VEGF	Hs.73793	Hs00173626_m1
Biglycan	Hs.821	Hs00156076_m1
Thrombomodulin	Hs.2030	Hs00264920_s1
EMMPRIN	Hs.501293	Hs00174305_m1
Versican	Hs.43488	Hs00171642_m1
Collagen VI alpha I	Hs.415997	Hs00242448_m1
TGF-B2	Hs.169300	Hs00236092_m1

This table lists the Applied Biosystems primer and probe identifier numbers and the Unigene ID for the target genes that were used for validation of the microarray analysis. Each identifier refers to a pre-developed assay reagent (PDAR) which contain the necessary PCR reagents including pre-designed forward and reverse primers for the target and control genes, pre-optimized in one solution for use with TaqMan™ universal PCR master mix. PDARs were obtained from Applied Biosystems by supplying the retrieved GenBank FASTA mRNA sequence for each target gene.

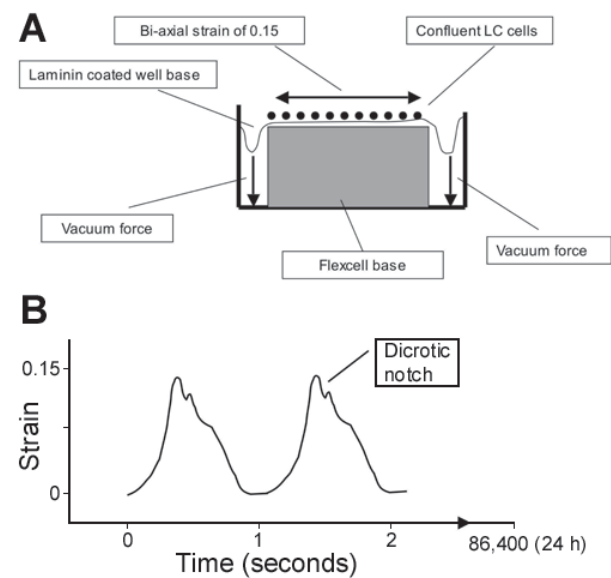


Figure 2. System for producing cyclical mechanical stretch. **A:** Schematic of a well from the 6 well Flexercell plates. Vacuum force draws the periphery of the well downwards and exerts a biaxial strain on confluent cells above the Flexercell base. **B:** Pattern of cyclical (1 Hz) mechanical stretch exposed to confluent lamina cribrosa (LC) cells. The stretch profile contains a dicrotic notch that is similar to the waveform in the pulsating central retinal artery. This was maintained for 24 h (86,400 cycles).

**Double immunofluorescence histochemistry:** EMMPRIN (green) and GFAP (red) immunoreactivity were both increased in the lamina cribrosa of glaucomatous tissue sections compared with the normal control sections. A representative micrograph is shown in Figure 6; glaucomatous lamina cribrosa tissue (Figure 6B), normal control lamina cribrosa tissue (Figure 6A). EMMPRIN protein was detected both distinct from, and co-localized (yellow) with GFAP in the glaucomatous sections. No staining was evident when the primary antibody was omitted (Figure 6C,D).

### DISCUSSION

In this study, using microarray technology, we investigated global gene expression in LC cells in response to 24 h of cyclical mechanical stretch. Our results illustrate that the transcriptional profile of mechanically induced genes in LC cells contains several components and modulators of the ECM (e.g., elastin, collagen IV, VI, VIII, IX, XIV, fibulin 1, thrombospondin 1, VEGF, ADAMTS2, ADAMTS9, MMP-23A, and lysyl oxidase). In order to validate the microarray

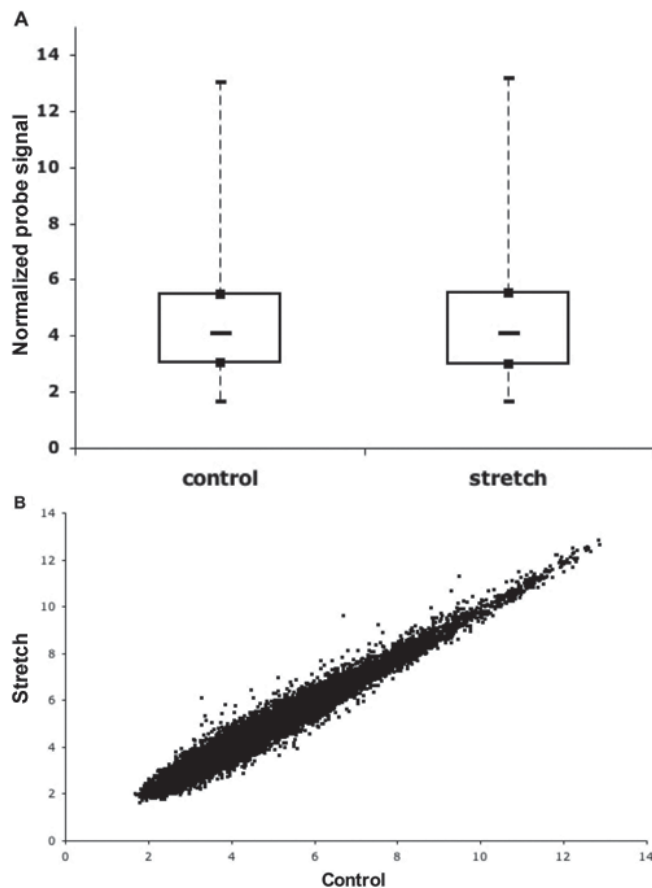


Figure 3. Summary of microarray analysis. **A:** Box plot distribution of average probe set expression levels as measured by robust multi-chip (RMA) analysis. The two microarrays are shown representing hybridization of pooled RNA from three separate stretch and control experiments. **B:** Scatter plot pairwise comparison of the log transformed and normalized expression levels of the 22,283 genes on the HG-U133A array.

results a number of genes were chosen for quantitative real time PCR analysis. This set of genes comprised eight upregulated (Collagen VI, elastin, TGF- $\beta$ 2, BMP-7, biglycan, versican, EMMPRIN, and VEGF) and one downregulated (thrombomodulin). They were selected because they are components or modulators of the ECM and as such may play a

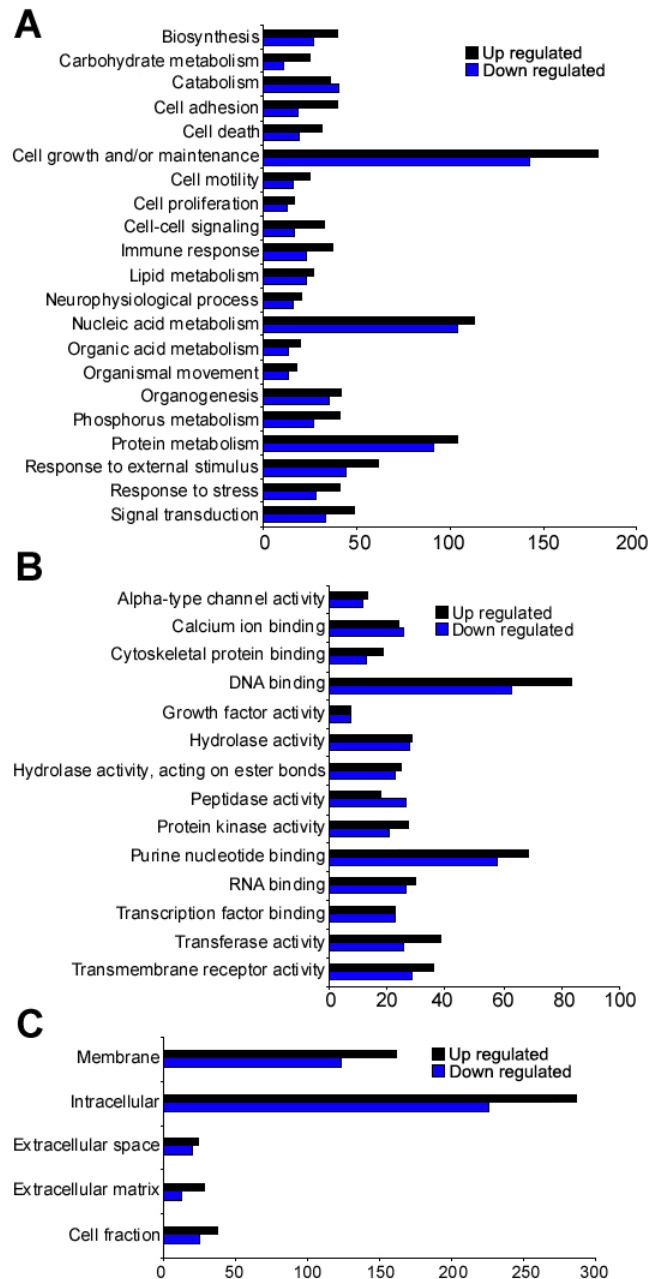


Figure 4. Ontology of stretch responsive genes. In order to generate biologically relevant groups of genes from the microarray data, we used the NIH DAVID version 1.0 software. This separated the data into three broad categories of biological process (A), molecular function (B), and cellular component (C). This analysis provides a generalized view of the global expression changes that took place in the LC cells following 24 h of cyclical mechanical stretching. Ontological categories are represented on the y-axis and the number of genes belonging to each category are represented on the x-axis.

TABLE 2. ONTOLOGY OF STRETCH RESPONSIVE GENES

Affymetrix probe ID	Gene	Fold	SLR
Extracellular matrix			
216269_s_at	elastin	8	3
201262_s_at	biglycan	3.7	1.9
212937_s_at	collagen, type VI, alpha 1	3	1.6
214535_s_at	ADAMTS2	2.6	1.4
220287_at	ADAMTS9	2.3	1.2
204724_s_at	collagen, type IX, alpha 3	2.3	1.2
205200_at	tetranectin (plasminogen binding protein)	2.3	1.2
205524_s_at	cartilage linking protein 1	2	1
216866_s_at	collagen, type XIV, alpha 1	2	1
207118_s_at	matrix metalloproteinase 23B	2	1
211571_s_at	versican (chondroitin sulfate proteoglycan 2)	1.9	0.9
201654_s_at	perlecan (heparan sulfate proteoglycan 2)	1.9	0.9
213640_s_at	lysyl oxidase	1.9	0.9
216339_s_at	tenascin XB	1.9	0.9
201107_s_at	thrombospondin 1	1.9	0.9
210628_x_at	latent transforming growth factor beta binding protein 4	1.7	0.8
205713_s_at	cartilage oligomeric matrix protein	1.7	0.7
211966_at	collagen, type IV, alpha 2	1.7	0.7
209156_s_at	collagen, type VI, alpha 2	1.7	0.7
204358_s_at	fibronectin leucine rich transmembrane protein 2	1.7	0.7
208005_at	netrin 1	1.7	0.7
220705_s_at	ADAMTS7	1.5	0.6
220677_s_at	ADAMTS8	1.5	0.6
221900_at	collagen, type VIII, alpha 2	1.5	0.6
207835_at	fibulin 1	-1.5	-0.6
202007_at	nidogen (enactin)	-1.5	-0.6
212667_at	secreted protein, acidic, cysteine-rich (osteonectin)	-1.5	-0.6
201843_s_at	EGF-containing fibulin-like extracellular matrix protein 1	-1.7	-0.8
203881_s_at	dystrophin	-2	-1
209758_s_at	Microfibril-associated glycoprotein-2	-2	-1
Cell proliferation			
203729_at	epithelial membrane protein 3	3.5	1.8
200973_s_at	transmembrane 4 superfamily member 8	3	1.6
214667_s_at	tumor protein p53 inducible protein 11	2.3	1.2
209468_at	low density lipoprotein receptor-related protein 5	2	1
211289_x_at	cell division cycle 2-like 1 (PITSLRE proteins)	2	1
208711_s_at	cyclin D1 (PRAD1: parathyroid adenomatosis 1)	1.9	0.9
203085_s_at	transforming growth factor, beta 1	1.7	0.8
209908_s_at	transforming growth factor, beta 2	1.7	0.8
201111_at	CSE1 chromosome segregation 1-like (yeast)	1.6	0.7
201419_at	BRCA1 associated protein-1	1.6	0.7
213977_s_at	CDKN1A interacting zinc finger protein 1	1.6	0.7
202253_s_at	dynamamin 2	1.5	0.6
210513_s_at	vascular endothelial growth factor	1.5	0.6
219708_at	5',3'-nucleotidase, mitochondrial	1.5	0.6
201641_at	bone marrow stromal cell antigen 2	-1.5	-0.6
204998_s_at	activating transcription factor 5	-1.5	-0.6
222243_s_at	transducer of ERBB2, 2	-1.5	-0.6
206341_at	interleukin 2 receptor, alpha	-1.6	-0.7
218386_x_at	ubiquitin specific protease 16	-1.6	-0.7
211297_s_at	cyclin-dependent kinase 7	-1.7	-0.8
205207_at	interleukin 6 (interferon, beta 2)	-1.9	-0.9
207358_x_at	microtubule-actin crosslinking factor 1	-1.9	-0.9
219049_at	chondroitin beta1,4 N-acetylgalactosaminyltransferase	-1.9	-0.9
202214_s_at	cullin 4B	-2	-1
202934_at	hexokinase 2	-2	-1

TABLE 2, CONTINUED.

Affymetrix probe ID	Gene	Fold	SLR
Growth factor activity			
209590_at	bone morphogenetic protein 7 (osteogenic protein 1)	1.6	0.7
206814_at	nerve growth factor, beta polypeptide	1.5	0.6
207595_s_at	bone morphogenetic protein 1	1.5	0.6
221577_x_at	growth differentiation factor 15	1.5	0.6
207865_s_at	bone morphogenetic protein 8b (osteogenic protein 2)	-1.5	-0.6
209961_s_at	hepatocyte growth factor (hepapoietin A; scatter factor)	-1.5	-0.6
206382_s_at	brain-derived neurotrophic factor	-1.6	-0.7
221404_at	interleukin 1 family, member 6 (epsilon)	-1.7	-0.8
210997_at	hepatocyte growth factor (hepapoietin A; scatter factor)	-2.6	-1.4
Cell surface receptor linked signal transduction			
208677_s_at	EMMPRIN/basigin (OK blood group)	2.5	1.3
213746_s_at	filamin A, alpha (actin binding protein 280)	2.5	1.3
208703_s_at	amyloid beta (A4) precursor-like protein 2	2.1	1.1
206534_at	glutamate receptor, ionotropic, N-methyl D-aspartate 2A	2	1
210594_x_at	myelin protein zero-like 1	2	1
208463_at	gamma-aminobutyric acid (GABA) A receptor, alpha 4	1.9	0.9
212196_at	interleukin 6 signal transducer (gp130, oncostatin M receptor)	1.9	0.9
207556_s_at	diacylglycerol kinase, zeta 104 kDa	1.7	0.8
211590_x_at	thromboxane A2 receptor	1.7	0.8
203882_at	interferon-stimulated transcription factor 3, gamma 48 kDa	1.6	0.7
204379_s_at	fibroblast growth factor receptor 3	1.6	0.7
205357_s_at	angiotensin II receptor, type 1	1.5	0.6
205977_s_at	EphA1	1.5	0.6
210651_s_at	EphB2	1.5	0.6
214391_x_at	prostaglandin E receptor 1 (subtype EP1), 42 kDa	1.5	0.6
220005_at	G protein-coupled receptor 86	1.5	0.6
200653_s_at	calmodulin 1 (phosphorylase kinase, delta)	-1.5	-0.6
200745_s_at	guanine nucleotide binding protein, beta polypeptide 1	-1.5	-0.6
204597_x_at	stanniocalcin 1	-1.5	-0.6
216837_at	EphA5	-1.5	-0.6
220336_s_at	glycoprotein VI (platelet)	-1.5	-0.6
204595_s_at	stanniocalcin 1	-1.6	-0.7
209071_s_at	regulator of G-protein signalling 5	-1.6	-0.7
216222_s_at	myosin X	-1.6	-0.7
219032_x_at	opsin 3 (encephalopsin, panopsin)	-1.6	-0.7
205168_at	discoidin domain receptor family, member 2	-1.7	-0.8
221299_at	super conserved receptor expressed in brain 3	-1.7	-0.8
202886_s_at	protein phosphatase 2, regulatory subunit A, beta isoform	-2	-1
214184_at	neuropeptide FF-amide peptide precursor	-2	-1
Coagulation			
201107_s_at	thrombospondin 1	1.9	0.9
209676_at	tissue factor pathway inhibitor	1.5	0.6
210049_at	serine proteinase inhibitor, clade C, member 1	1.5	0.6
211668_s_at	plasminogen activator, urokinase	1.5	0.6
200986_at	serine proteinase inhibitor, clade G, member 1	-1.5	-0.6
207808_s_at	protein S (alpha)	-1.5	-0.6
220336_s_at	glycoprotein VI (platelet)	-1.5	-0.6
213380_x_at	macrophage stimulating 1	-1.9	-0.9
201860_s_at	plasminogen activator, tissue	-2	-1
203887_s_at	thrombomodulin	-3	-1.6

This table lists the ontological categories (and their member genes) as generated by the NIH DAVID version 1.0 software. The individual categories of ECM, cell proliferation, growth factor activity, cell surface receptor linked signal transduction, and coagulation are shown here as they are the categories to which the 9 validated genes belong. Of particular interest to our work was the ECM category, which showed that 30 ECM genes were differentially expressed in stretch and control (24 upregulated, 6 downregulated).

role in ECM remodeling in the optic nerve head in POAG. Three of the validated genes, collagen VI, elastin, and TGF-β2 have previously been characterized in the optic nerve head in POAG. The remaining six validated genes are, to our knowledge, novel in the context of ECM remodeling in POAG.

The parameters used in these experiments were 15% biaxial strain at 1 Hz maintained for 24 h. These are standard parameters that have been used extensively by other investigators using other cell types [25]. The cyclic component (1 Hz) corresponded to ocular pulsations and the dicrotic waveform produced by the Flexercell apparatus created a physiological approximation to the central retinal artery pressure waveform (Figure 2B). A mathematical model of lamina cribrosa stresses in raised IOP as generated by Edwards et al. [26] demonstrated that the lamina cribrosa will experience strain of 12% at 40 mm Hg. While this relationship was not linear it is possible that the 15% strain used in our experiments could emulate the effect of pressures in excess of 40 mm Hg. Though these conditions are not an exact reproduc-

tion of the microenvironment to which LC cells are exposed in raised IOP in vivo, the Flexercell system does produce stimuli that are useful to investigators of POAG in vitro.

We chose a ±0.6 signal log ratio (±1.5 fold) cut off to filter the microarray data because the quantile normalization method of RMA which we used produces comparatively smaller signal log ratios than does the average scaling method of Affymetrix MAS 5.0 [23]. Briefly, the differences between the analysis methods relates to background correction, Affymetrix MAS 5.0 uses a large background correction which adds more noise but gives larger fold change estimates. RMA gives smaller fold change estimates because smaller background corrections are made, but with minimal noise and more precision [27].

Collagen fibers constitute an important fraction of the human lamina cribrosa ECM. The center of each cribriform plate is composed of collagen I, III, V, and VI, surrounded by a layer of basement membrane type IV collagen to which the LC cells are attached [28,29]. Collagens behave in a synergis-

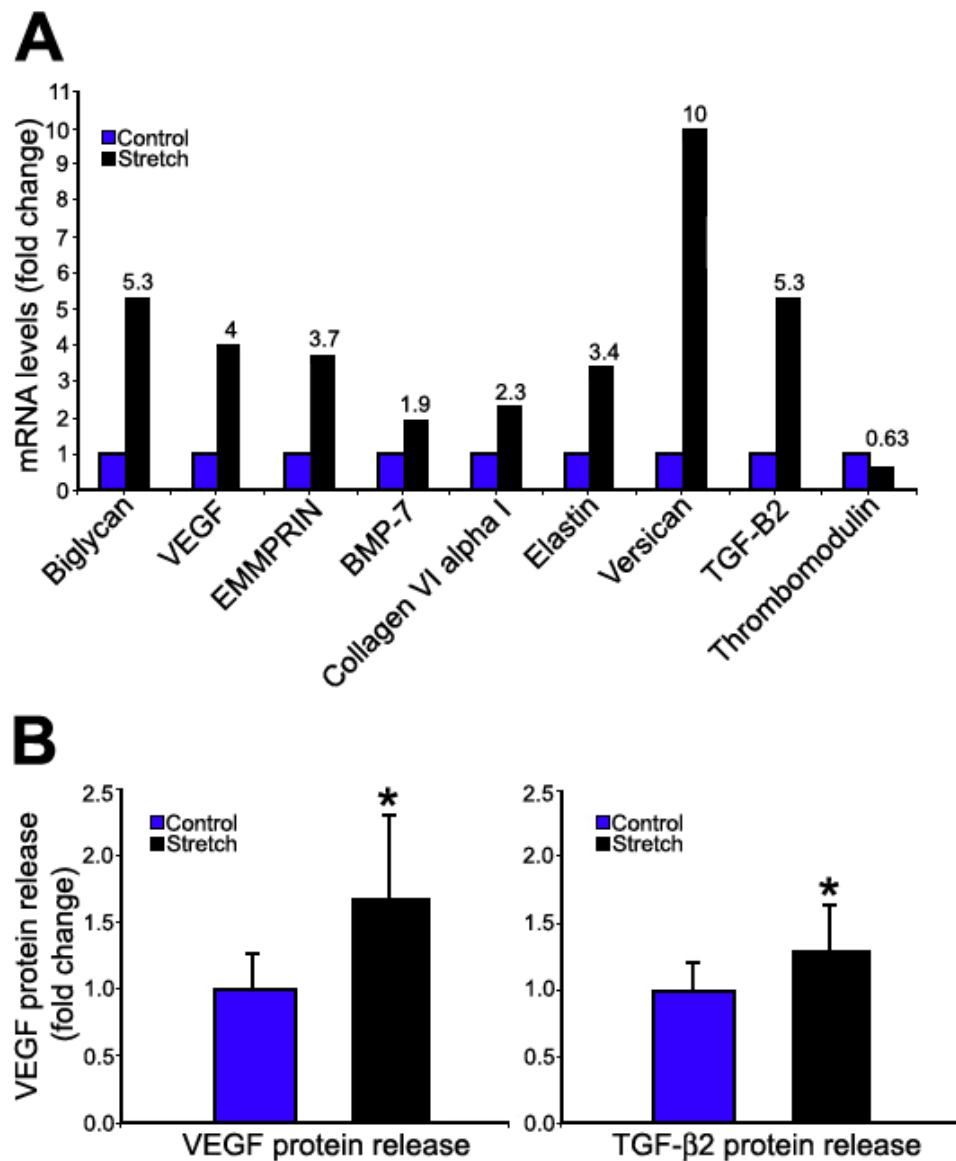


Figure 5. Validation of microarray analysis. **A:** Nine genes whose expression was upregulated (biglycan, VEGF, EMMPRIN, BMP-7, collagen VI alpha1, elastin, versican, and TGF-β2) or downregulated (thrombospondin) in response to cyclical mechanical stretch were analyzed in independent experiments by real-time TaqMan PCR. The direction of expression changes in these genes was reproducible and consistent with microarray analysis. **B:** ELISA investigated if changes in mRNA synthesis reflected similar changes in protein production. VEGF and TGF-β2 were chosen as representative genes whose expression was altered by cyclical mechanical stretch. VEGF and TGF-β2 protein secretion was significantly increased in cell media supernatants of stretched lamina cribrosa cells compared to static controls (n=4). Mean control VEGF concentration was 241±66 pg/ml and mean stretch VEGF concentration was 407±148 pg/ml (n=4; p=0.03). Mean control TGF-β2 concentration was 87±19 pg/ml and mean stretch TGF-β2 concentration was 115±30 pg/ml (n=4; p=0.02). The asterisks indicate a statistically significant difference in protein secretion between stretched and control groups.

tic manner with elastic fibers, and are thought to provide structural support to the lamina cribrosa and adjacent RGC axons [30]. Another function of collagen VI is the organization of fibronectin protein in the ECM [31]. Marked elevation in collagen VI protein has been demonstrated in the lamina cribrosa tissue of both monkeys with experimentally elevated IOP and humans with POAG [32,33]. Collagen type I and basement membrane type IV collagen are also increased in the lamina cribrosa in POAG [30]. Our finding that LC cells upregulate collagen IV and VI expression in response to mechanical stretch is, therefore, important and indicates that this cell type may be a source for this protein in POAG. The other collagens which were upregulated by stretch were collagen VIII, IX, and XIV. These collagens may also play a role in ECM changes in the glaucomatous lamina cribrosa and provide new targets for immunohistochemistry studies of optic nerve head tissue.

Elastin, like collagen, is a major component of the lamina cribrosa ECM and is typically found in tissues that are exposed to mechanical stresses *in vivo* [34]. Elastin is a classically upregulated protein in many fibrotic diseases, and in the glaucomatous lamina cribrosa, its fibers become curled and their architecture deranged, in a process referred to as elastotic degeneration [35]. It is likely that the changes in optic nerve head elastin metabolism in POAG reflect a response to chronic

elevation of IOP. Support for this comes from studies of experimental IOP elevation in monkeys where increased production of morphologically abnormal elastin has been shown in the lamina cribrosa of experimental animals, but not in normal IOP controls [36]. *In vitro* studies using human optic nerve head astrocytes exposed to hydrostatic pressure have also shown that both elastin mRNA and protein expression are upregulated after 24 h in this environment [15]. It may, therefore, be the case that elastotic degeneration adversely affects the lamina cribrosa's intrinsic compliance, predisposing it to collapse and compression as IOP rises. Two other genes that were downregulated in our system, MAGP-2 and fibulin-1, encode important proteins involved in elastin fiber assembly in the ECM [37,38] and also may be important in the disturbed elastin production that occurs in the glaucomatous lamina cribrosa.

TGF- $\beta$ 2, a member of the TGF- $\beta$  superfamily, is a multifunctional cytokine whose biological activities include induction of ECM synthesis, modulation of wound healing, and inhibition of cell growth [39]. While the prototypical isoform, TGF- $\beta$ 1, has been detected in normal adult human lamina cribrosa tissue, TGF- $\beta$ 2 is the predominant type found in this tissue in POAG [12]. In this setting, it may be responsible for the progressive accumulation and remodelling of the lamina

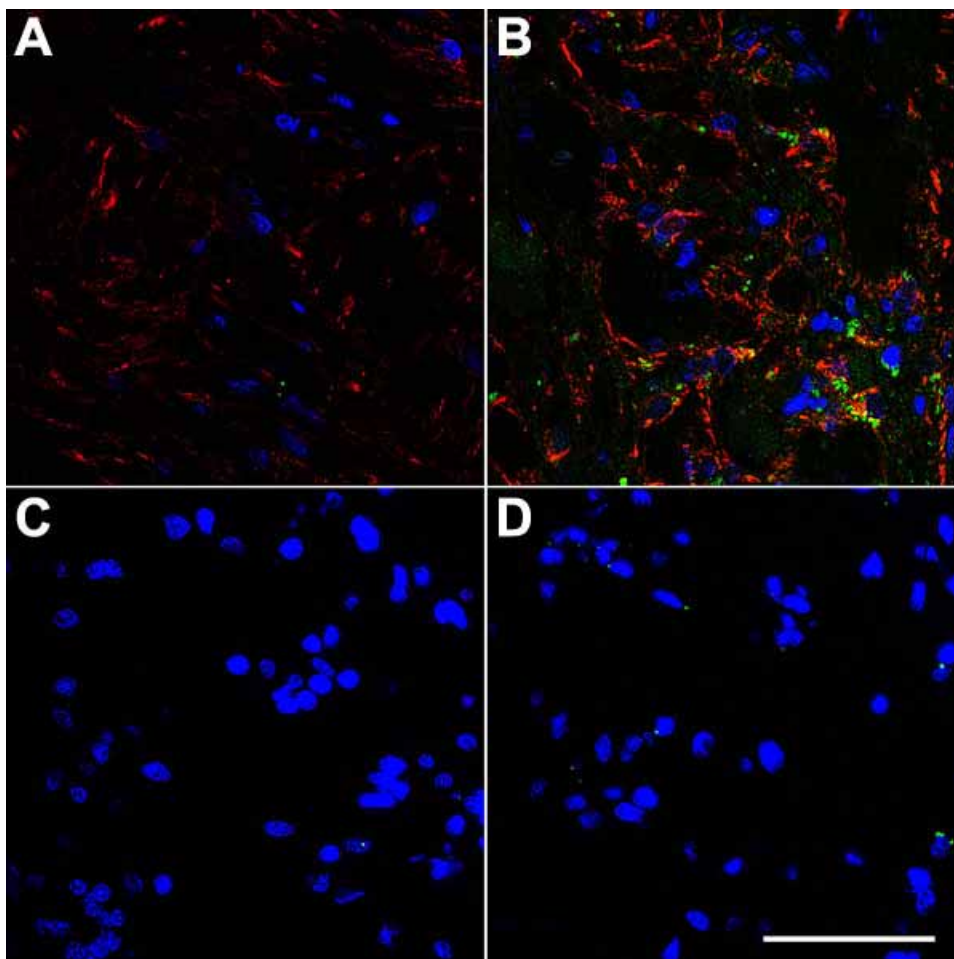


Figure 6. Double immunofluorescence histochemistry of normal and glaucomatous human optic nerve head tissue. Normal (A) and glaucomatous (B) optic nerve head sections were stained for EMMPRIN (green) and GFAP (red). EMMPRIN and GFAP staining were markedly increased in the glaucomatous sections compared to the normal controls. EMMPRIN was detected separate from and co-localized with GFAP (yellow) in the glaucomatous sections. Cell nuclei were DAPI stained (blue). No immunostaining was seen in the absence of primary antibody (C,D). The scale bar (D) represents 50  $\mu$ m.

cribrosa ECM as demonstrated by immunohistochemistry studies [40]. We found both TGF- $\beta$ 2 mRNA and TGF- $\beta$ 2 protein expression to be increased in LC cells exposed to 24 h of cyclical mechanical stretch. We also found that TGF- $\beta$ 1 mRNA was upregulated in response to mechanical stretch, therefore, indicating that LC cells may be a significant source of TGF- $\beta$ 1 and TGF- $\beta$ 2 in the lamina cribrosa in POAG, possibly in response to the mechanical stimulus of raised IOP.

Bone morphogenetic proteins (BMPs) are also members of the TGF- $\beta$  superfamily [41]. They were originally detected as bone and cartilage inducing proteins but their other functions include regulation of developmental processes such as cell proliferation and apoptosis [42]. Human LC cells in vitro express mRNA and protein for BMP-2, BMP-4, BMP-7, and the BMP receptor complex [43]. Like their family members TGF- $\beta$ 1 and TGF- $\beta$ 2, cyclical mechanical stretch also upregulated the synthesis of BMP-1 and BMP-7 mRNA in our study. BMP-1 has been shown to modulate the formation of collagen I fibers and BMP-7 possesses anti-fibrotic properties [44,45]. Taken in this context, stretch induced BMP-1 and BMP-7 mRNA synthesis in LC cells may represent a response intended to modulate ECM accumulation in the optic nerve head.

Proteoglycans are another important component of the mammalian ECM and are present in both the human and monkey lamina cribrosa [46,47]. Elevated chondroitin sulfate proteoglycans are also evident in the lamina cribrosa of monkeys with laser-induced glaucoma, but not in normal IOP controls [48]. This may represent a compensatory response to elevated IOP, as the expandable hydrodynamic volume which proteoglycans can generate is thought to aid buffering of intraocular/cerebrospinal fluid (translaminar) pressure gradients [30]. We found that the expression of three proteoglycans, perlecan, biglycan, and versican were upregulated in LC cells in response to cyclical mechanical stretch. Perlecan is a heparan sulfate proteoglycan and a major component of basement membranes and functions in anchoring other matrix proteins to the basal lamina [49]. Biglycan is a member of the family of small matrix proteoglycans which includes decorin and fibromodulin. It has several functions including extracellular organization of collagen VI fibers and support of neuronal growth [50]. Versican is a large proteoglycan belonging to the hyaluronan-binding family that includes aggrecan and neurocan. Expression of the V3 isoform of versican was upregulated by stretch in our experiments. Versican V3 can induce tropoelastin synthesis in arterial smooth muscle cells and correct impaired elastogenesis in fibroblasts [51,52]. These findings indicate that mechano-responsive perlecan, biglycan, and versican V3 expression may be relevant to basement membrane, collagen VI, and elastin metabolism in the ONH in POAG.

EMMPRIN (extracellular matrix metalloproteinase inducer) is a transmembrane glycoprotein and a member of the immunoglobulin superfamily. Its functions include induction of anchorage independent cell proliferation and stimulation of matrix metalloproteinase-2 (MMP-2) activity [53-55]. We found that EMMPRIN mRNA synthesis was upregulated in

response to mechanical stretch in LC cells and that there was a marked increase in EMMPRIN protein staining in glaucomatous lamina cribrosa tissue compared to normal controls. EMMPRIN was identified distinct from, and co-localized with, GFAP in the glaucomatous sections. This staining pattern appears to indicate that both astrocytes and GFAP-negative cells (i.e., LC cells) may be responsible for upregulation of this MMP inducing protein in POAG. This is the first study examining EMMPRIN in the human optic nerve head, and we believe that its detection there is of relevance to the characteristic ECM changes in the glaucomatous lamina cribrosa. As mentioned above, EMMPRIN can induce anchorage-independent cell growth, which it achieves via a hyaluronan-dependent mechanism. This property of EMMPRIN may be important to reactive astrocytes in the glaucomatous optic nerve head, which in CNS injuries detach from their basement membranes and migrate to and proliferate at sites of axonal damage [56].

Thrombomodulin, another transmembrane glycoprotein, demonstrated downregulation in response to mechanical stretch in LC cells. This negative transcriptional response in the thrombomodulin gene has also been shown in human vascular smooth muscle cells exposed to mechanical strain in vitro [57]. During experimental wound healing, heterozygous thrombomodulin deficient mice exhibit thicker and denser foci of collagen aggregates than wild type controls [58]. As mentioned above, collagen VI deposition is increased in the lamina cribrosa in POAG. However, collagen I and IV are similarly elevated and form compacted bundles of fibers that are unlike those in normal tissue [59]. That thrombomodulin expression was reduced in stretched LC cells is intriguing, and may contribute to an explanation for the disorganized collagen deposition that occurs in the lamina cribrosa in POAG.

VEGF is an established angiogenic, pro-proliferative growth factor whose transcription is driven by several stimuli such as mechanical strain and hypoxia [60,61]. VEGF induces a number of ECM remodelling enzymes including members of the MMP family [62]. It also drives the expression of connective tissue growth factor (CTGF), a potent mediator of fibrosis, ECM synthesis, and angiogenesis [63]. More recently, VEGF has been suggested as an important neurotrophic and neuroprotective agent in the central and peripheral nervous systems [64]. For instance, it can stimulate axonal outgrowth in superior cervical and dorsal root ganglion cells and migration of astrocytes in vitro. We found that both VEGF mRNA synthesis and VEGF protein release were upregulated in LC cells following 24 h of cyclical mechanical stretch. It is possible that in POAG, stretch-induced VEGF may promote ECM remodeling, modulate astrocyte activity, and support RGC axon survival.

Our data shows consistency with previous in vitro studies conducted by Cui et al. [65] on human scleral fibroblasts and Yang et al. [66] on ONH astrocytes where microarray analysis identified similarly stretch responsive genes (e.g., VEGF and elastin). In contrast to the latter study, however, our results appear to show more transcription of ECM genes in LC cells than in ONH astrocytes, though it is acknowledged that the stretching methods were different in both studies. Other

work conducted by Ahmed et al. [67] examined transcriptional patterns in retinal tissue from rats which had been exposed to chronically elevated IOP. Microarray analysis showed that expression of VEGF and several other ECM components (fibronectin and SPARC) and modulators (TIMP-1 and MMP-3) were upregulated in the experimental retinas compared with normal IOP controls. In common with our earlier work measuring TGF- $\beta$ 1 mRNA synthesis using real time PCR [18], this gene was also unregulated (Table 2, cell proliferation) in this present study. Though we had also found that MMP-2 protein activity was significantly increased in LC cells following 24 h of mechanical stretching, we did not observe similar changes at the mRNA level in the present study. Taken together, our data and those of these preceding studies strongly suggests that mechanical forces in the optic nerve head and retina are important in inducing ECM synthesis and turnover.

To our knowledge this study represents the first broad gene expression analysis of LC cells exposed to cyclical mechanical stretch. The data indicates that the LC cell's transcriptional response to mechanical stretch may be intended to bolster the lamina cribrosa's ECM, ultimately preventing its collapse during extended periods of elevated IOP. This represents an additional step towards understanding the role and mechanism of mechanical stretch stimuli in the optic nerve head in POAG. Future work will determine the precise pathological stimulus to which LC cells should be exposed, either varying the degree (e.g., <15%) or chronicity (e.g., >24 h) of strain. We also believe that our results provide new candidate ECM proteins to detect in glaucomatous optic nerve head tissue, proteins which may bear relevance to the pathogenesis of POAG (e.g., EMMPRIN). Finally, this study highlights a likely role for LC cells and mechanical stimuli in ONH ECM metabolism, particularly as LC cells express alpha smooth muscle actin and are, therefore, primed to respond to external stimuli in a pro-fibrotic manner [5]. Our results also give sufficient rationale for investigating the anti-fibrotic and possible therapeutic potential of interrupting LC cell responses to mechanical stimuli in POAG.

#### ACKNOWLEDGEMENTS

Ruaidhrí P. Kirwan is supported by a grant from the Mater College for Post Graduate Education and Research 2003-2004. The authors wish to acknowledge the advice and technical assistance of William Howe, Debbie Lane (Glaucoma Research, Alcon Research Ltd., Fort Worth, TX), Anne-Marie Brun, and Dr. Lawrence Oakford (UNTHSC at Fort Worth, Fort Worth, TX).

#### REFERENCES

- Anderson DR. Ultrastructure of human and monkey lamina cribrosa and optic nerve head. *Arch Ophthalmol* 1969; 82:800-14.
- Albon J, Purslow PP, Karwatowski WS, Easty DL. Age related compliance of the lamina cribrosa in human eyes. *Br J Ophthalmol* 2000; 84:318-23.
- Albon J, Karwatowski WS, Easty DL, Sims TJ, Duance VC. Age related changes in the non-collagenous components of the extracellular matrix of the human lamina cribrosa. *Br J Ophthalmol* 2000; 84:311-7.
- Hernandez MR, Igoe F, Neufeld AH. Cell culture of the human lamina cribrosa. *Invest Ophthalmol Vis Sci* 1988; 29:78-89.
- Lambert W, Agarwal R, Howe W, Clark AF, Wordinger RJ. Neurotrophin and neurotrophin receptor expression by cells of the human lamina cribrosa. *Invest Ophthalmol Vis Sci* 2001; 42:2315-23.
- Hernandez MR. The optic nerve head in glaucoma: role of astrocytes in tissue remodeling. *Prog Retin Eye Res* 2000; 19:297-321.
- Quigley HA, Hohman RM, Addicks EM, Massof RW, Green WR. Morphologic changes in the lamina cribrosa correlated with neural loss in open-angle glaucoma. *Am J Ophthalmol* 1983; 95:673-91.
- Quigley HA. Number of people with glaucoma worldwide. *Br J Ophthalmol* 1996; 80:389-93.
- Coleman AL, Quigley HA, Vitale S, Dunkelberger G. Displacement of the optic nerve head by acute changes in intraocular pressure in monkey eyes. *Ophthalmology* 1991; 98:35-40.
- Levy NS, Crapps EE. Displacement of optic nerve head in response to short-term intraocular pressure elevation in human eyes. *Arch Ophthalmol* 1984; 102:782-6.
- Hernandez MR. Ultrastructural immunocytochemical analysis of elastin in the human lamina cribrosa. Changes in elastic fibers in primary open-angle glaucoma. *Invest Ophthalmol Vis Sci* 1992; 33:2891-903.
- Pena JD, Taylor AW, Ricard CS, Vidal I, Hernandez MR. Transforming growth factor beta isoforms in human optic nerve heads. *Br J Ophthalmol* 1999; 83:209-18.
- Quigley HA, Addicks EM. Chronic experimental glaucoma in primates. II. Effect of extended intraocular pressure elevation on optic nerve head and axonal transport. *Invest Ophthalmol Vis Sci* 1980; 19:137-52.
- Bellezza AJ, Rintalan CJ, Thompson HW, Downs JC, Hart RT, Burgoyne CF. Deformation of the lamina cribrosa and anterior scleral canal wall in early experimental glaucoma. *Invest Ophthalmol Vis Sci* 2003; 44:623-37.
- Hernandez MR, Pena JD, Selvidge JA, Salvador-Silva M, Yang P. Hydrostatic pressure stimulates synthesis of elastin in cultured optic nerve head astrocytes. *Glia* 2000; 32:122-36.
- Salvador-Silva M, Ricard CS, Agapova OA, Yang P, Hernandez MR. Expression of small heat shock proteins and intermediate filaments in the human optic nerve head astrocytes exposed to elevated hydrostatic pressure in vitro. *J Neurosci Res* 2001; 66:59-73.
- Yang JL, Neufeld AH, Zorn MB, Hernandez MR. Collagen type I mRNA levels in cultured human lamina cribrosa cells: effects of elevated hydrostatic pressure. *Exp Eye Res* 1993; 56:567-74.
- Kirwan RP, Crean JK, Fenerty CH, Clark AF, O'Brien CJ. Effect of cyclical mechanical stretch and exogenous transforming growth factor-beta1 on matrix metalloproteinase-2 activity in lamina cribrosa cells from the human optic nerve head. *J Glaucoma* 2004; 13:327-34.
- Liu B, Neufeld AH. Expression of nitric oxide synthase-2 (NOS-2) in reactive astrocytes of the human glaucomatous optic nerve head. *Glia* 2000; 30:178-86.
- Hernandez MR, Agapova OA, Yang P, Salvador-Silva M, Ricard CS, Aoi S. Differential gene expression in astrocytes from human normal and glaucomatous optic nerve head analyzed by cDNA microarray. *Glia* 2002; 38:45-64.
- Wordinger RJ, Lambert W, Agarwal R, Liu X, Clark AF. Cells of the human optic nerve head express glial cell line-derived neu-

- rotrophic factor (GDNF) and the GDNF receptor complex. *Mol Vis* 2003; 9:249-56.
22. Banes AJ, Gilbert J, Taylor D, Monbureau O. A new vacuum-operated stress-providing instrument that applies static or variable duration cyclic tension or compression to cells in vitro. *J Cell Sci* 1985; 75:35-42.
  23. Bolstad BM, Irizarry RA, Astrand M, Speed TP. A comparison of normalization methods for high density oligonucleotide array data based on variance and bias. *Bioinformatics* 2003; 19:185-93.
  24. Dennis G Jr, Sherman BT, Hosack DA, Yang J, Gao W, Lane HC, Lempicki RA. DAVID: Database for Annotation, Visualization, and Integrated Discovery. *Genome Biol* 2003; 4:P3.
  25. WuDunn D. The effect of mechanical strain on matrix metalloproteinase production by bovine trabecular meshwork cells. *Curr Eye Res* 2001; 22:394-7.
  26. Edwards ME, Good TA. Use of a mathematical model to estimate stress and strain during elevated pressure induced lamina cribrosa deformation. *Curr Eye Res* 2001; 23:215-25.
  27. Irizarry RA, Bolstad BM, Collin F, Cope LM, Hobbs B, Speed TP. Summaries of Affymetrix GeneChip probe level data. *Nucleic Acids Res* 2003; 31:e15.
  28. Hernandez MR, Wang N, Hanley NM, Neufeld AH. Localization of collagen types I and IV mRNAs in human optic nerve head by in situ hybridization. *Invest Ophthalmol Vis Sci* 1991; 32:2169-77.
  29. Ye H, Yang J, Hernandez MR. Localization of collagen type III mRNA in normal human optic nerve heads. *Exp Eye Res* 1994; 58:53-63.
  30. Hernandez MR, Pena JD. The optic nerve head in glaucomatous optic neuropathy. *Arch Ophthalmol* 1997; 115:389-95.
  31. Sabatelli P, Bonaldo P, Lattanzi G, Braghetta P, Bergamin N, Capanni C, Mattioli E, Columbaro M, Ognibene A, Pepe G, Bertini E, Merlini L, Maraldi NM, Squarzone S. Collagen VI deficiency affects the organization of fibronectin in the extracellular matrix of cultured fibroblasts. *Matrix Biol* 2001; 20:475-86.
  32. Fukuchi T. [Extracellular matrix of the optic nerve lamina cribrosa in monkey eyes with experimentally induced glaucoma]. *Nippon Ganka Gakkai Zasshi* 1991; 95:303-10.
  33. Hernandez MR, Andrzejewska WM, Neufeld AH. Changes in the extracellular matrix of the human optic nerve head in primary open-angle glaucoma. *Am J Ophthalmol* 1990; 109:180-8.
  34. Xu C, Zarins CK, Glagov S. Gene expression of tropoelastin is enhanced in the aorta proximal to the coarctation in rabbits. *Exp Mol Pathol* 2002; 72:115-23.
  35. Pena JD, Netland PA, Vidal I, Dorr DA, Rasky A, Hernandez MR. Elastosis of the lamina cribrosa in glaucomatous optic neuropathy. *Exp Eye Res* 1998; 67:517-24.
  36. Quigley HA, Brown A, Dorman-Pease ME. Alterations in elastin of the optic nerve head in human and experimental glaucoma. *Br J Ophthalmol* 1991; 75:552-7.
  37. Penner AS, Rock MJ, Kielty CM, Shipley JM. Microfibril-associated glycoprotein-2 interacts with fibrillin-1 and fibrillin-2 suggesting a role for MAGP-2 in elastic fiber assembly. *J Biol Chem* 2002; 277:35044-9.
  38. Roark EF, Keene DR, Haudenschild CC, Godyna S, Little CD, Argraves WS. The association of human fibulin-1 with elastic fibers: an immunohistological, ultrastructural, and RNA study. *J Histochem Cytochem* 1995; 43:401-11.
  39. Yu L, Border WA, Huang Y, Noble NA. TGF-beta isoforms in renal fibrogenesis. *Kidney Int* 2003; 64:844-56.
  40. Yan X, Tezel G, Wax MB, Edward DP. Matrix metalloproteinases and tumor necrosis factor alpha in glaucomatous optic nerve head. *Arch Ophthalmol* 2000; 118:666-73.
  41. Yamashita H, Ten Dijke P, Heldin CH, Miyazono K. Bone morphogenetic protein receptors. *Bone* 1996; 19:569-74.
  42. Hogan BL. Bone morphogenetic proteins: multifunctional regulators of vertebrate development. *Genes Dev* 1996; 10:1580-94.
  43. Wordinger RJ, Agarwal R, Talati M, Fuller J, Lambert W, Clark AF. Expression of bone morphogenetic proteins (BMP), BMP receptors, and BMP associated proteins in human trabecular meshwork and optic nerve head cells and tissues. *Mol Vis* 2002; 8:241-50.
  44. Ge G, Seo NS, Liang X, Hopkins DR, Hook M, Greenspan DS. Bone morphogenetic protein-1/tolloid-related metalloproteinases process osteoglycin and enhance its ability to regulate collagen fibrillogenesis. *J Biol Chem* 2004; 279:41626-33.
  45. Morrissey J, Hruska K, Guo G, Wang S, Chen Q, Klahr S. Bone morphogenetic protein-7 improves renal fibrosis and accelerates the return of renal function. *J Am Soc Nephrol* 2002; 13:S14-21.
  46. Sawaguchi S, Iwata K, Kaiya T. [The distribution and characterization of sulfated-proteoglycans in the normal human lamina cribrosa]. *Nippon Ganka Gakkai Zasshi* 1991; 95:311-7.
  47. Morrison JC, Rask P, Johnson EC, Deppmeier L. Chondroitin sulfate proteoglycan distribution in the primate optic nerve head. *Invest Ophthalmol Vis Sci* 1994; 35:838-45.
  48. Fukuchi T, Sawaguchi S, Yue BY, Iwata K, Hara H, Kaiya T. Sulfated proteoglycans in the lamina cribrosa of normal monkey eyes and monkey eyes with laser-induced glaucoma. *Exp Eye Res* 1994; 58:231-43.
  49. Irving-Rodgers HF, Harland ML, Rodgers RJ. A novel basal lamina matrix of the stratified epithelium of the ovarian follicle. *Matrix Biol* 2004; 23:207-17.
  50. Wiberg C, Heinegard D, Wenglen C, Timpl R, Morgelin M. Biglycan organizes collagen VI into hexagonal-like networks resembling tissue structures. *J Biol Chem* 2002; 277:49120-6.
  51. Merrilees MJ, Lemire JM, Fischer JW, Kinsella MG, Braun KR, Clowes AW, Wight TN. Retrovirally mediated overexpression of versican v3 by arterial smooth muscle cells induces tropoelastin synthesis and elastic fiber formation in vitro and in neointima after vascular injury. *Circ Res* 2002; 90:481-7.
  52. Hinek A, Braun KR, Liu K, Wang Y, Wight TN. Retrovirally mediated overexpression of versican v3 reverses impaired elastogenesis and heightened proliferation exhibited by fibroblasts from Costello syndrome and Hurler disease patients. *Am J Pathol* 2004; 164:119-31.
  53. Marieb EA, Zoltan-Jones A, Li R, Misra S, Ghatak S, Cao J, Zucker S, Toole BP. Emmprin promotes anchorage-independent growth in human mammary carcinoma cells by stimulating hyaluronan production. *Cancer Res* 2004; 64:1229-32.
  54. Caudroy S, Polette M, Nawrocki-Raby B, Cao J, Toole BP, Zucker S, Birembaut P. EMMPRIN-mediated MMP regulation in tumor and endothelial cells. *Clin Exp Metastasis* 2002; 19:697-702.
  55. Li R, Huang L, Guo H, Toole BP. Basigin (murine EMMPRIN) stimulates matrix metalloproteinase production by fibroblasts. *J Cell Physiol* 2001; 186:371-9.
  56. Rhodes KE, Moon LD, Fawcett JW. Inhibiting cell proliferation during formation of the glial scar: effects on axon regeneration in the CNS. *Neuroscience* 2003; 120:41-56.
  57. Feng Y, Yang JH, Huang H, Kennedy SP, Turi TG, Thompson JF, Libby P, Lee RT. Transcriptional profile of mechanically induced

- genes in human vascular smooth muscle cells. *Circ Res* 1999; 85:1118-23.
58. Peterson JJ, Rayburn HB, Lager DJ, Raife TJ, Kealey GP, Rosenberg RD, Lentz SR. Expression of thrombomodulin and consequences of thrombomodulin deficiency during healing of cutaneous wounds. *Am J Pathol* 1999; 155:1569-75.
59. Morrison JC, Dorman-Pease ME, Dunkelberger GR, Quigley HA. Optic nerve head extracellular matrix in primary optic atrophy and experimental glaucoma. *Arch Ophthalmol* 1990; 108:1020-4.
60. Leonard MO, Cottell DC, Godson C, Brady HR, Taylor CT. The role of HIF-1 alpha in transcriptional regulation of the proximal tubular epithelial cell response to hypoxia. *J Biol Chem* 2003; 278:40296-304.
61. Petersen W, Varoga D, Zantop T, Hassenpflug J, Mentlein R, Pufe T. Cyclic strain influences the expression of the vascular endothelial growth factor (VEGF) and the hypoxia inducible factor 1 alpha (HIF-1alpha) in tendon fibroblasts. *J Orthop Res* 2004; 22:847-53.
62. Unemori EN, Ferrara N, Bauer EA, Amento EP. Vascular endothelial growth factor induces interstitial collagenase expression in human endothelial cells. *J Cell Physiol* 1992; 153:557-62.
63. Suzuma K, Naruse K, Suzuma I, Takahara N, Ueki K, Aiello LP, King GL. Vascular endothelial growth factor induces expression of connective tissue growth factor via KDR, Flt1, and phosphatidylinositol 3-kinase-akt-dependent pathways in retinal vascular cells. *J Biol Chem* 2000; 275:40725-31.
64. Sondell M, Lundborg G, Kanje M. Vascular endothelial growth factor has neurotrophic activity and stimulates axonal outgrowth, enhancing cell survival and Schwann cell proliferation in the peripheral nervous system. *J Neurosci* 1999; 19:5731-40.
65. Cui W, Bryant MR, Sweet PM, McDonnell PJ. Changes in gene expression in response to mechanical strain in human scleral fibroblasts. *Exp Eye Res* 2004; 78:275-84.
66. Yang P, Agapova O, Parker A, Shannon W, Pecan P, Duncan J, Salvador-Silva M, Hernandez MR. DNA microarray analysis of gene expression in human optic nerve head astrocytes in response to hydrostatic pressure. *Physiol Genomics* 2004; 17:157-69.
67. Ahmed F, Brown KM, Stephan DA, Morrison JC, Johnson EC, Tomarev SI. Microarray analysis of changes in mRNA levels in the rat retina after experimental elevation of intraocular pressure. *Invest Ophthalmol Vis Sci* 2004; 45:1247-58.